Regression Analysis Studies of Polymer Transitions II. T_{ll} from Specific Heat and Other Data for Polyisobutylene

RAYMOND F. BOYER, *Michigan Molecular Institute, 1910 West St. Andrews Road, Midland, Michigan 48640* and JOHN B. ENNS, *AT&T Bell Laboratories, Whippany, New Jersey 07981*

Synopsis

Linear regression analysis studies with residuals of heat capacity vs. temperature (C_p vs. T) data above the glass transition temperature (T_g) for polyisobutylene (PIB) of molecular weights $\overline{M}_v$ = 1,350,000 and M = 4900 show that the data points can be represented by three straight lines in each case. The lower intersection temperature represents the intermolecular T_{ll} transition (relaxation); the upper one an intramolecular T_{ll}, process. Both processes are confirmed by ultrasonic velocity data in vulcanized butyl rubber, by zero shear melt viscosity data in PIB (M = 4900); and by isothermal specific volume vs. pressure data in PIB ($\overline{M}_v$ = 36,000). T_{ll} is confirmed by thermal diffusivity, differential scanning calorimetry (DSC), ^{13}C nuclear magnetic resonance (NMR) spectroscopy and the T* temperature of Lobanov and Frenkel based on Arrhenius-type plots (log frequency vs. $1/T_g$). A comparison of dynamic mechanical loss data, both old and new, reveal that T_{ll} follows a Vogel-WLF type relation; log f vs. $1/(T_{ll} - 1/T_0)$. PIB samples with number average molecular weights between 7100 to 860,000 have been measured on three types of support systems: glass braid (0.3 Hz), filter paper (11 Hz), brass shim stock (14-16 Hz), and give similar values of T_{ll}. A considerable amount of literature data long neglected from the viewpoint of its bearing on T_{ll} is reviewed. T_{ll} has been observed in the same way as T_g by both relaxational and quasi-static methods. Some instructive cross comparisons between these two types of methods emerge. With so many diverse methods yielding evidence for T_{ll} in PIB, it cannot be dismissed as an artifact. A molecular origin for T_{ll} is plausible in terms of the Frenkel-Baranov phase dualism mechanism. A complete relaxation map (log f vs. $1/T$) has been assembled with frequencies from 10^{-2} to 10^{10} Hz and temperatures from 150 to 500 K. It shows T_β, T_g, T_{ll} and methyl group rotation, all based on data in the literature. The molecular weight dependence of T_g and T_{ll} and the low resiliency of butyl rubber as it relates to T_{ll} are discussed in the appendices.

INTRODUCTION

The first paper in this series[1] developed a systematic procedure based on available statistical techniques to analyze data (Y = F(T)) in the temperature region of known or suspected polymer transitions. These techniques were then applied to volume vs. temperature data of polycycloalkylmethacrylates using the published results of Wilson and Simha.[2] The existence of a liquid–liquid transition, T_{ll}, lying above the glass transition temperature, T_g, in these polymers, as suggested in Ref. 2, was demonstrated.[1] The present paper begins by extending these same procedures to adiabatic calorimeter data of Furakawa and Reilly on a classical, much investigated polymer, polyisobutylene (PIB).[3] The main point to be resolved by the regres-

Journal of Applied Polymer Science, Vol. 32, 4075–4107 (1986)
 CCC 0021-8995/86/034075-33$04.00

sion analysis techniques of Ref. 1 is that the two sets of tabulated data provided by Furakawa and Reilly lead to two different interpretations:

First, a set of raw data at irregular temperature intervals on which they did not comment. We have examined these raw data on several prior occasions[4-6] with the conclusion that heat capacity vs. temperature (C_p vs. T) plots above T_g consisted of two straight lines connected by curvature with a projected intersection at or about 265 K, which temperature we considered to represent the T_{ll} transition for this polymer. (For general background on T_{ll}, several reviews may be consulted.[7-10]) The first study[4] involved a hand-drawn plot of C_p vs. T values with straight lines drawn by visual inspection. The second study[5] employed crude regression analysis to characterize the two lines, and also collected collateral evidence for the existence of T_{ll} in PIB. A later study[6] offered still additional physical evidence to support the existence of a liquid–liquid event in PIB. This paper[6] placed T_{ll} near 240 K.

Second, a smoothed set of heat capacity (C_p) values at 5 K intervals which they reported to follow a quadratic above T_g:

$$C_p \text{ (J/gK)} = 0.844 \pm 3.03 \times 10^{-3} \times T + 2.29 \times 10^{-6} \times T^2 \quad (1)$$

Attention was also directed[5] to C_p vs. T data of Ferry and Parks[11] on a PIB of 4900 molecular weight which seemed to support the existence of T_{ll}: this set of data is re-examined with improved computer techniques because it helps to clarify the interpretation of the Furakawa and Reilly data.

Since these earlier studies,[4-6] several developments have occurred which merit a reexamination of PIB. Regression analysis techniques have been refined not only over those used in the earlier studies but also over those employed in Ref. 1, notably with an automatic method to search for intersections in Y = F(X) where F(X) consists of 2 to 10 linear segments.[12] New lines of physical evidence supporting the existence of T_{ll} in PIB have appeared, notably by ^{13}C NMR spectroscopy[13] and from analysis of isothermal volume-pressure data.[14] Evidence has been accumulating to suggest the presence of two liquid–liquid transitions, T_{ll} and $T_{l\rho}$, in several polymers, notably polystyrene (PS),[10,14,15] isotactic polymethylmethacrylate (PMMA)[12,16] and poly-*n*-butylmethacrylate.[17,18] T_{ll} at $(1.2 \pm 0.05) \times T_g$ is considered to arise from intermolecular effects, $T_{l\rho}$ at T_{ll} + (30 to 50 K) to arise from intramolecular barriers to rotation.[10,15] (Note: $T_{l\rho}$ was designated as $T_{ll'}$ in earlier literature before its nature was elucidated. A recent account appears in a review by one of us.[38])

Several recent developments have revealed new information about the liquid state of polymers and may provide direct evidence for T_{ll}. Sillescu and co-workers have reported several NMR studies on partially deuterated PS's.[19-21] They found a temperature region in which motion of the phenyl group about the chain backbone became as facile as motion about the phenyl-carbon bond. In one experiment an Arrhenius plot (log relaxation time τ vs. 1/T) for ring-deuterated PS (see Figure 8 of Ref 21) consisted of two straight lines, or perhaps two curved sections, intersecting at $\approx$ 195°C. While this behavior was previously linked with T_{ll},[21] it may show $T_{l\rho}$ instead, based on the very short relaxation times involved as well as collateral evidence from dielectric, NMR, ESR, and dynamic mechanical data discussed next.

Törmälä et al, using ESR data[22] and Lobanov and Frenkel, employing dielectric and mechanical loss data[23] have prepared relaxation maps for log f or log τ vs. $1/T_g$ and $1/T_\beta$. The log τ vs. $1/T_g$ plots exhibit a sharp decrease in slope at temperatures well above T_g (static) and at frequencies near 10^6 Hz or corresponding relaxation time, τ. Both groups of authors recognize that T_g and T_β type motions become similar in nature, i.e. both very local, at temperatures above this kink. Lobanov and Frenkel label this kink T* and relate it to T_{ll}. These results will be amplified in the section on relaxation maps.

Because of these general indications for both T_{ll} and $T_{l\rho}$, the several sets of data subjected to regression analysis earlier[5,6] have now been reexamined by more refined techniques. Evidence for both T_{ll} and $T_{l\rho}$ has been found.

In addition to the general developments discussed above, three new techniques for locating T_{ll} by dynamic mechanical loss have been described. Cowie and McEwen[24–26] have tested polymer impregnated filter paper under tension in the Rheovibron at frequencies ranging from 3.5 to 110 Hz. T_{ll} was observed in several oligomers and polymers, one of which was PIB.[26]

A second method developed by Starkweather and Giri[27] employs polymer-coated metal shim stock in the DuPont 981 dynamic mechanical analyzer. It involves the deformation of specimens in flexure. We have refined their technique to study the liquid state of polymers, including PIB, at least 100 K above T_g.[28] Data of this type will be discussed later.

The third method forms a dispersion of PIB particles in a continuous matrix of PS. This composite specimen is then measured in the DuPont DMA apparatus. A T > T_g loss peak corresponding to T_{ll} was found.[29] This method depends on the fact that T_{ll}(PIB) < T_g(PS).

Finally, a molecular level hypothesis advanced by Frenkel and Baranov (see pages 540 to 542 of Ref. 10) to explain T_{ll} seems generally consistent with known facts about T_{ll}. Segment–segment interaction is opposed by a gain in the entropy of the macromolecule as temperature increases. The segment–segment component is increased by chain stiffness, polarity, and hydrostatic pressure; decreased by diluent. T_{ll} is weakened in some test methods by cross-linking which restricts macromolecular mobility.

Regarding nomenclature, we speak of T_{ll} as a transition because of its many similarities to T_g. T_{ll} does depend on frequency and hence has a relaxational character just as T_g does. Some may prefer to designate T_{ll} as a relaxation. Less is known about the nature of the $T_{l\rho}$.

In addition to these specific new developments, it was inevitable that continued perusal of the literature should lead to significant bodies of data hitherto overlooked. These will be introduced at appropriate places.

THE C_p DATA OF FURAKAWA AND REILLY

Furakawa and Reilly[3] used a 40.736 g specimen of PIB with $\overline{M}_v$ = 1,350,000, and $\overline{M}_w$ = 1,560,000 Daltons. Since their smoothed data were represented by Eq. (1) whereas the raw data seemed to us to follow two straight lines[4–6] a reexamination of both sets of data by the objective methods discussed in Ref. 1 seemed desirable.

We have thereby confirmed the quadratic character of the smoothed C_p vs. T data, with the following result:

$$C_p \text{ (J/gk)} = 0.84422 + 3.0348 \times 10^{-3} + 2.2400 \times 10^{-6}T^2 \quad \text{(1a)}$$

with a standard error in C_p (calculated) of 0.27826×10^{-3} J/gK which is 0.0142% error at midrange of C_p (at 300 K). The correlation coefficient, R^2, is unity. The extra significant figures in Eq. (1a) are shown to emphasize the excellent agreement with the original analysis given as Eq. (1). Our computer program provides a graph of RES/SE $\hat{Y}$ as a function of T where RES signifies a residual (RES = C_p (observed) − C_p (calculated)) and SE $\hat{Y}$ is the standard error in $\hat{Y}$ where $\hat{Y}$ is C_p (calculated). Details about such RES/SE $\hat{Y}$ plots are summarized in Ref. 1 and discussed in standard texts on modern statistical procedures.[30,31] In the RES/SE $\hat{Y}$ plot shown in Figure 1, the pattern is seemingly random about zero, with points falling within ±2 standard errors. The validity of the quadratic model appears confirmed, although a sequence of 5 points from 250 to 270 K inclusive and another sequence of 6 points from 295 to 315 K inclusive are distinctly nonrandom about zero.

Figure 2 is the RES/SE $\hat{Y}$ plot for the raw data using a quadratic model. We now note that the pattern is distinctly nonrandom although the standard error in C_p (calculated) is 0.52367×10^{-2} J/gK which is 0.266% at 302 K. $R^2 = 0.99947$. We further note that the sequence of 8 negative RES/SE $\hat{Y}$ values from 233 to 302 K is markedly nonrandom. The equation for the

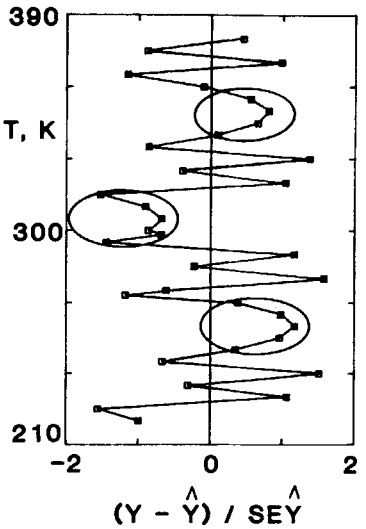

Fig. 1. [Residuals (RES)]/[standard error in $\hat{Y}$ (calculate) (SE $\hat{Y}$)] using a quadratic regression model for smoothed C_p vs. T data of Furakawa and Reilly[3] at T > T_g of PIB, $\overline{M}_v$ = 1,350,000, showing apparent randomness which indicates of a good fit. Note encircled nonrandom regions near 235, 300, and 345 K.

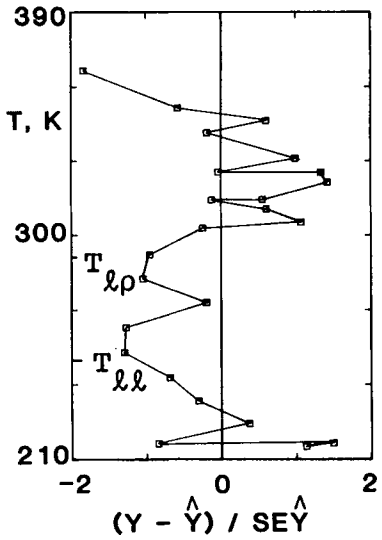

Fig. 2. RES/SE $\hat{Y}$ for quadratic regression model applied to raw C_p vs. T data of Furakawa and Reilly, showing nonrandom pattern and hence an incorrect fit. The expected location of T_{ll} and $T_{l\rho}$ from Figure 3 are indicated.

quadratic fit is

$$C_p(\text{rawdata}) = 0.86101 + 2.8975 \times 10^{-3} \times T + 2.5073 \times 10^{-5} \times T^2 \quad (2)$$
$$R^2 = 0.99988, \text{SE}\,\hat{Y} = 0.19549 \times 10^{-2}$$

The standard error is 7 times larger than for the smoothed data. Note that the raw data points at 215.78 K and 377.14 K seem to be in error, based on visual inspection of computer plots of C_p vs. T. Both were discarded, leaving 24 data points for the quadratic analysis given in Eq. (2), and for additional regression studies to be discussed later.

Following procedures recommended in Ref. 1, a linear least-squares model was applied to the raw C_p vs. T data. The RES/SE $\hat{Y}$ pattern appears in Figure 3 and is distinctly nonrandom as expected. It offers the possibility of two interpretations. Extension of the two straight lines gives an intersection at circa 271 K which we interpreted on an earlier occasion as T_{ll}.[4] However, there is an additional straight line extending from 252.99 to 292.23 K with five data points. Figure 3 resembles the standard RES/SE $\hat{Y}$ pattern for three straight lines shown as line D, Figure 3, of Ref. 1. This suggests a double transition: T_{ll} at 253 K and $T_{l\rho}$ at 292 K, separated by 39 K, similar to the temperature difference between T_{ll} and $T_{l\rho}$ found for higher molecular weight PS's. (See Figure 5 of Ref. 10 or Figure 1 of Ref. 15). Before making this assignment we applied a linear regression line to the C_p data of Ferry and Parks[11] with the RES/SE $\hat{Y}$ pattern seen in Figure 4. The similarity between Figures 3 and 4 is remarkable. The automatic intersection search method detailed in Ref. 12 placed the intersection temperatures at 236.0 and 265.7 K which we now assign as T_{ll} and $T_{l\rho}$ with a Δ T above T_{ll} of 30 K. These transition temperatures are lower than for Figure 4 as they should

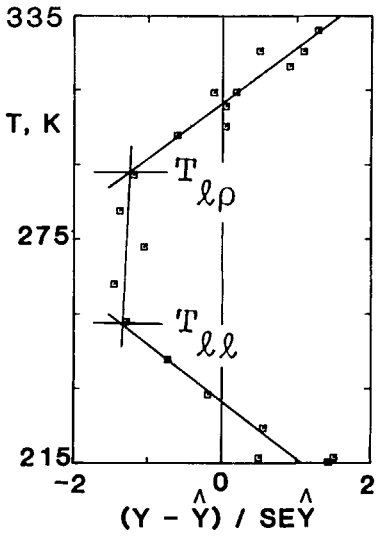

Fig. 3. RES/SE $\hat{Y}$ pattern for a linear model applied to raw C_p data of Furakawa and Reilly, with T_{ll} and $T_{l\rho}$ at the indicated temperatures. This pattern suggests three straight lines as a correct fit.

be because of the lower molecular weight and the Δ T is smaller for the same reason, consistent with the pattern found for PS (Fig. 5 of Ref. 10).

An earlier study[5] of this Ferry and Parks data, made before our regression analysis techniques were improved, showed a quadratic fit to be marginally better than two straight lines, based on standard errors. Because all data points are used in a quadratic while only a third of the points are used in each of the three lines, the quadratic fit is still marginally superior in terms

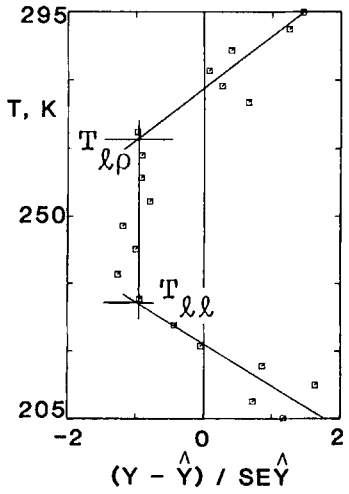

Fig. 4. RES/SE $\hat{Y}$ for a linear model applied to the C_p vs. T data of Ferry and Parks[11] at $T > T_g$ for PIB of M = 4900. T_{ll} and $T_{l\rho}$ are indicated.

of standard error. However, the RES/SE $\hat{Y}$ pattern (not shown) is clearly nonrandom for a quadratic model, especially near 236 K.

Even with agreement about $T_{l\rho}$ from two sets of C_p data we were still reluctant to accept its existence until additional evidence was found in other types of data to be examined later.

We suggested earlier[6] that T_{ll} might be as low as 240 K based on a computerized running first-derivative plot of the raw C_p vs. T data from Ref. 3. We later learned that this derivative program leads to distortion (false intersections) near one or both ends of a run if there are too few data points below a transition. Hence we have relied only on the residuals method in the present paper.

Two general comments about the Furakawa and Reilly C_p data seem pertinent: (a) While smoothing of the raw data gave an excellent quadratic fit by the normal standards of R^2 and small standard error, only the more sophisticated residuals method detected nonrandom behavior in a transition region. The RSE/SE $\hat{Y}$ plot showed that smoothing did not obliterate evidence for a transition. (b) Even though the raw data consisted of three linear segments, the computer generated a plausible quadratic fit with reasonable coefficients, high R^2 and small standard error. Again, the power of the residuals method showed that this quadratic model was in error. A cubic model was also tested on the raw data. In this case the signs of the coefficients were alternating and the residuals were very nonrandom in the transition region.

One cannot help wonder how many sets of literature data of diverse type, smoothed or otherwise, have been incorrectly categorized as following a polynomial fit when the residuals technique would rule otherwise. We have demonstrated that an R^2 approaching unity is no guarantee that the model tested provides a correct description of the data.

OTHER EVIDENCE FOR T_{ll}

As emphasized in Ref 1, even when a regression analysis study of the type just presented suggests an apparent anomaly in a set of data such as the slope changes in C_p, this is basically a commentary on that set of data but does not prove the existence of a transition(s). Nor can one argue *a priori* that the original authors were wrong in smoothing their data and arriving at a quadratic representation. They may have suspected the presence of an artifact resulting from any of several causes. However, if a transition (relaxation) is real, it should manifest itself in other types of physical evidence. Preliminary attempts to summarize such collateral evidence appeared in Refs. 5 and 6. Since Ref. 6 was submitted, new types of physical measurements have appeared in the literature and/or have been provided from MMI laboratory, as mentioned in the introduction.

In view of the numerous, extensive and diverse studies on PIB over the past 40 years, with sometimes conflicting or confusing results, reviewing such collateral data is indeed a formidable task. Nevertheless, we now attempt a definitive survey of the facts. We find ample evidence by a variety of methods to support the existence of T_{ll} and $T_{l\rho}$.

There is, we suggest, a hierarchy of data types starting with the most rigorous, as follows:

1. Thermodynamic data
   a. other C_p data
   b. thermal diffusivity
   c. isobaric V vs. T at P = 1 atm.
   d. ultrasonic sound velocity
   e. isothermal V-P data at P > 1 atm.
2. NMR data
3. Dielectric data
4. Dynamic mechanical analysis data
5. Zero shear melt viscosity

This progression, while somewhat arbitrary, proceeds from quasiequilibrium thermodynamics type data to relaxational or viscoelastic studies. The data will be discussed in the order outlined above. The supportive C_p vs. T data of Ferry and Parks[11] has already been discussed in connection with Figure 4.

DIFFERENTIAL SCANNING CALORIMETRY

Plots of C_p vs T above T_g as examined earlier[4–6] showed an endothermic slope change at T_{ll}, as confirmed by the residuals patterns of Figures 3 and 4. Figure 5 shows a recent trace of a 7.24 mg specimen of $\overline{M}_n$ = 7900 on a more sensitive instrument, the DuPont DSC 990-910 unit at a sensitivity setting of 0.5 mV/cm, and a heating rate of 10 K/min. The specimen had previously been heated to 200°C, held isothermally at that temperature for 15 minutes, and free cooled to room temperature. No slope change was observed in the baseline obtained using empty sample pans. An endothermic slope change at 246 K, with T_g at 209 K gives a T_{ll}/T_g ratio of 1.18. $T_{l\rho}$ was not observed.

DSC should be the most direct test of our conclusion about the slope change above T_g. However, at the high sensitivity needed to observe T_{ll}, artifacts are possible and hence we prefer to have additional supporting evidence.

THERMAL DIFFUSIVITY

A method closely related to C_p is the measurement of thermal diffusivity, $\alpha = \lambda/\rho C_p$, where λ is thermal conductivity, ρ is density, and C_p is specific heat. Ueberreiter has a method for measuring α directly as a function of temperature. He consistently finds step decreases in α at T_g and at $T > T_g \approx 1.2\ T_g$, both a function of $\overline{M}_n$ for a variety of polymers. We have examined his study of α in PMMA on two occasions (Figure 2, Ref. 9 and Figure 10 of Ref. 10).

For PIB of unspecified molecular weight he observed a $T > T_g$ transition at 252 K. He ascribed it to the onset of methyl group rotation but, as we shall mention in connection with Figure 15, such a motion sets in close to 0 K. We assign this event to T_{ll}.

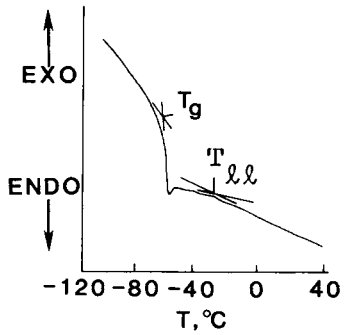

Fig. 5. DSC trace at 10 K/min on PIB on $\overline{M}_n$ = 7100 with DuPont 990-910 DSC at a heating rate of 10 K/min sensitivity of 0.5 mV/cm, sample weight of 7.24 mg, empty reference pan. T_{ll} is shown as an endothermic slope change. T_g = −64°C, T_{ll} = −27°C, T_{ll}/T_g (K/K) = 1.18.

VOLUME VS. TEMPERATURE DATA

Ferry and Parks[11] plotted coefficients of expansion for their PIB specimen of 4900 molecular weight up to 300 K. However, the scatter in the data above T_g is very great, as typical for point to point derivatives. There is no evidence for T_{ll} or $T_{l\rho}$.

Bekkedahl[34] gave tabulated mercury dilatometer data on a specimen of vulcanized butyl rubber gum stock from 249 to 355 K. V_{sp} is strictly linear as a function of temperature over this temperature interval and hence there is no verification on the existence of $T_{l\rho}$. T_{ll} would be at or below the lowest measured temperature. We have not located any other V vs. T data on either PIB or butyl rubber.

ULTRASONIC SOUND VELOCITY

This topic is closely related to thermal expansion. Work[35] has reviewed evidence showing that an abrupt decrease in the temperature coefficient of ultrasonic velocity, dv_s/dT, at T_g (static) is a consequence of the sudden change in coefficients of expansion at T_g, since $v_s = \sqrt{E/\rho}$. We have recently shown for different polymers (but not PIB) that there is a discontinuity in the coefficient of thermal expansion at T_{ll}, similar in nature but much smaller than the one at T_g[18]. It thus seemed possible that dv_s/dT should decrease at the static T_{ll} temperature. While examining the ultrasonic attenuation data of Ivey et al.[36] to determine the effect of frequency on T_g (see Figure 15) we noted, especially from their Figure 3, the variation of sound velocity with temperature at five frequencies from 4.4×10^4 to 10^7 Hz. The curves at higher frequencies seemed to suggest a slope decrease near −25°C, far above T_g (static) and in fact essentially at T_{ll} (static) for a lightly vulcanized unfilled butyl rubber.

Since no data points were shown in Ref. 36, we then studied the doctoral dissertation of Ivey[37] which did present the data points. Figure 6 is a replot of v_s vs. T at 10^7 Hz. In the thesis these points were fitted by smoothed curves but we suggest that the fits shown by us giving slope changes for both T_{ll} and $T_{l\rho}$ at 10^7 Hz are more in accord with evidence presented in

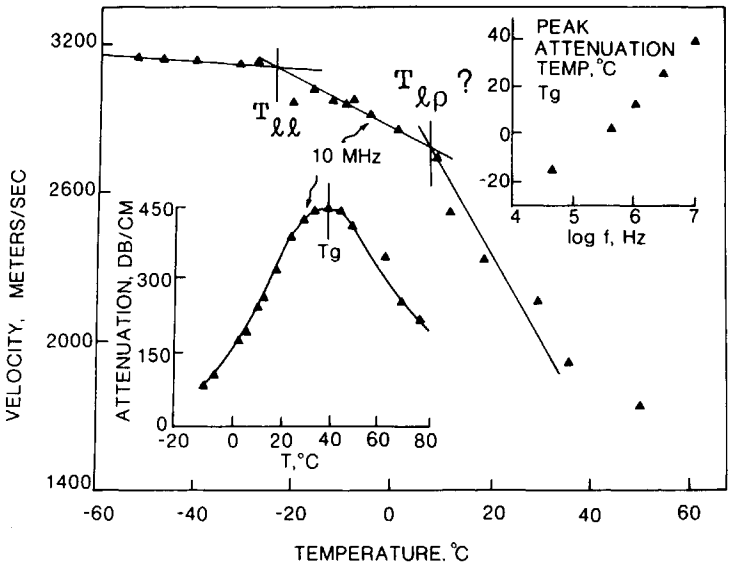

Fig. 6. Bulk wave velocity for vulcanized butyl rubber gum stock: 10^7 Hz (From Fig. 9 of Ref. 37. A comparison of all frequencies but without data points is shown in Figure 3 of Ref. 36. Insets: Bottom, attenuation in db/cm. at 10^7 Hz. The peak temperature is T_g for 10^7 Hz. Top, increase in T_g with frequency.

our paper. These intersections give static values for T_{ll} and $T_{l\rho}$. The lower left insert to Figure 6 is a plot of attenuation vs. temperature at 10^7 Hz and the upper right insert is a plot of T_g vs. frequency. We suggest that the T_g loss process at the lower frequencies interferes with observation of $T_{l\rho}$ in the v_s vs. T curve.

Our interpretation gains credence not only from the good agreement of T_{ll} and $T_{l\rho}$ with other static values assembled later in Table II but also from similar slope changes for Heavea at -31°C and SBR at -28°C, again at 10^7 Hz on vulcanized unfilled systems.[38] As a precautionary note, the numerical values of the slope changes at 10 MHz are larger than one would expect from a change in thermal expansion, as if the T_g dispersion process were contributing to it. There may also be a contribution from other dispersions such as the abrupt decrease in modulus at T_{ll} recently found by Maxwell (see Appendix III).

Thurn[39] has presented data showing T_{ll} directly at ultrasonic frequencies but this will be covered in the section on relaxation maps (Figure 15).

ISOTHERMAL VOLUME-PRESSURE DATA

An early study of isothermal V-P data on several polymers presented the locus of T_{ll} for PIB in the T-P plane, with a pressure coefficient of 120 K/kbar, the highest one yet known.[14] Various refinements in regression analysis, coupled with the use of a linear form of the Tait equation which treats volume as a function of pressure, required a new study of PIB. Evidence for both T_{ll} and $T_{l\rho}$ were found. Since many subissues not germane to the present paper were involved this entire topic will be covered elsewhere. Figure 7

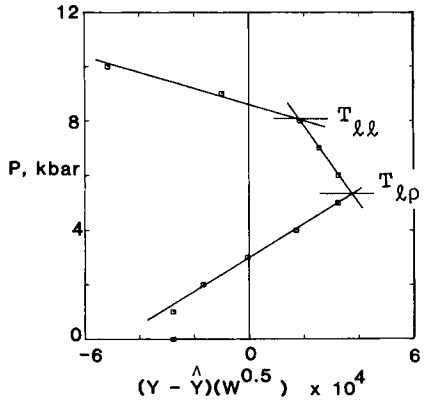

Fig. 7. RES/SE $\hat{Y}$ for linear Tait equation fit to isothermal V-P data of Beret and Prausnitz[40] at 84.5°C, showing pressures for T_{ll} and $T_{l\rho}$. W is a weighting factor recommended by Solc et al.[12] to give a uniform weight at all pressures.

shows the residuals pattern for the 84.5°C isotherm with indications of T_{ll} and $T_{l\rho}$ as marked: the viscosity average molecular weight of the specimen used was 36,000.

In the new technique used to obtain Figure 7, $y = f(P)$ is plotted using isothermal V-P data with

$$y = \exp[(1/C)(1 - V/V_0)] - 1 = (P - P_0)/b \tag{3}$$

where P is hydrostatic pressure in bars, V is the measured volume in cc/g at P, V_0 its value at P_0. C is a constant for the entire isotherm, while b increases stepwise at each pressure-induced transition; in this case, T_{ll} and $T_{l\rho}$. Details of the method appear in Ref. 12.

It may appear inconsistent that T_{ll} was not observed in V vs. T data but was found in P-V-T data. Actually, it was detected in isothermal V vs. P data at temperatures more than 100 K above T_{ll} at $P_0 = 1$ atm, where isothermal compressibility, κ, is relatively large.[41] T_{ll} shows up as a slope change in κ vs. P when hydrostatic pressure induces the transformation from the super-liquid state to the liquid state, just above T_g. Similar remarks hold for $T_{l\rho}$.

NMR DATA

Axelson and Mandelkern determined ^{13}C NMR spectra for several polymers including PIB.[42] They reported a characteristic temperature, T_c, at which these spectra collapsed on cooling, with $T_c > T_g$. We later presented evidence that $T_c \equiv T_{ll}$.[13] T_c for PIB on a specimen of unspecified molecular weight was given as 263 K.

Thurn[39] has presented a curve showing the half width of the proton resonance signal vs. temperature for PIB of molecular weight 1,750,000 with T_g at 263 K and a $T > T_g$ process at 307 K (ratio of 1.17). The change in half width for this latter process is only 0.4 Gauss compared with a decrease of about 8 Gauss at T_g. We consider this $T > T_g$ process to be T_{ll} raised to

this high temperature by the high NMR frequency. While the exact frequency is not stated, it is likely in the range of 10^5 to 10^6 Hz.[39a] This point falls on the line for T_{ll} from tan δ in Figure 15.

DIELECTRIC BEHAVIOR OF PIB

Even though PIB is relatively nonpolar with a dipole moment of only 0.08 Debye, Stoll et al.[43] have presented dielectric loss, tan δ, as a function of frequency (their Figure 20), and as a function of temperature from about −190 to about 125°C at frequencies of 25 to 50 Hz (their Figure 21). The specimen was Oppanol 15 of molecular weight about 100,000. The main peak is T_g. However, there is clear cut evidence for two loss processes below T_g which they label δ and δ′ (see Figure 15 later).

There is a very weak shoulder above T_g about which they do not comment but which may correspond to T_{ll} or a combined T_{ll} and $T_{l\rho}$. It may correspond to the dynamic mechanical loss peak above T_g which they also found, as will be discussed in the next section.

DYNAMIC MECHANICAL LOSS

We consider nine different sets of dynamic mechanical loss data on PIB and/or butyl rubber as follows:

1. The torsion pendulum data of Schmieder and Wolf on several PIB's.[44]
2. J″ vs. T[45] and J″ vs. log ωa_T[46] data of Ferry et al., based on the use of the Fitzgerald appartus which subjects the specimen to vibratory shear deformation.
3. The J″ shear compliance data of Stoll et al.[43] on a 4,700,000 molecular weight PIB over a wide range of frequency and temperature, confirming the data of Item 2. The type of apparatus was not specified.
4. Data on butyl rubber by Sanders and Ferry,[47] with the Fitzgerald apparatus.
5. Data of Kramer et al.[50] on PIB as a guest polymer in vulcanized butyl rubber (Fitzgerald apparatus).
6. Torsional braid analysis (TBA) data on six different PIB's by Wei and Gillham.[51]
7. Several PIB's[28] measured by the DuPont dynamic mechanical analyzer (DMA) with the shim stock technique of Starkweather and Giri.[27]
8. Rheovibron data using filter paper support.[26]
9. DMA analysis of PIB encapsulated in PS.[29]

These nine sets do not exhaust the literature resources but were intended to demonstrate that different support systems for the liquid state of PIB, different deformation modes, a range of frequencies, and different loss functions have been investigated.

1. Schmieder and Wolf[44] employed a hanging torsion pendulum with PIB's of molecular weight 500,000, 900,000, and 1,750,000. There was the start of a $T > T_g$ loss peak for the lowest molecular weight and several loss peaks for the two highest. We suggest that these peaks might be T_{ll} or $T_{l\rho}$. Their

loss curve on unvulcanized butyl rubber likewise showed a double loss peak above T_g.

2. Fitzgerald et al.[45] presented tan δ = J″/J′ plots as a function of temperature at several frequencies. There was a double loss peak corresponding to T_g and T > T_g evident at 400 Hz. We show this as Figure 8A. Figure 8B is the comparison plot of J″/J′ as a function of log ωa_T given in Figure 5 of Ferry et al.[46] (ω is the angular frequency, a_T the reduction factor).

Fitzgerald et al.[45] did not attach a label to the T > T_g loss peak of Figure 8A, although they did emphasize that the T > T_g peak was not the result of an artifact and that it was unique to PIB, not being observed in PS and PVC. We have identified the $T > T_g$ peak with T_{ll} in Refs. 4 and 5, and also in Figure 20 of Ref. 10.

The location of the two peaks is naturally reversed in Figure 8B compared to Figure 8A. Because of its position with respect to T_g, it was subsequently referred to by Ferry and his students as "the slow process," and ascribed to the slippage of untrapped dangling entanglements.[47] Ferry and his students seem to have adopted the Figure 8B representation exclusively (Refs. 47 and 48, for example) but Figure 8A is the more common practice.

The behavior shown in Figure 8A and B should be typical of T_g and T_{ll} for all polymers. We have shown a similar comparison for polybutadiene (Figure 3 of Ref. 10) where the T_{ll} peak is weaker than the T_g peak.

Ref. 45 contains a table of J′ and J″ values as a function of temperature and frequency. Figure 9 is a plot of J′ and J″ against temperature at 600 Hz showing their pattern in the T > T_g region. Such plots can be prepared from 60 to 600 Hz inclusive but the peak in J″ is off scale at lower and higher frequencies. Tan δ = J″/J′ can be calculated over a wide frequency range.

We have shown[6] that J″ vs. T plots exhibit maxima which shift in the expected manner with frequency (see Figure 2 of Ref. 6, Figure 20 of Ref. 10). We also noted[6] that in Figure 10.24 of McCrum et al.,[54] the locus of the log f – $1/T_{max}$ map, where T_{max} is the temperature of J''_{max}, was T > T_g. The correct locus for T_g appeared as the tan δ curve.

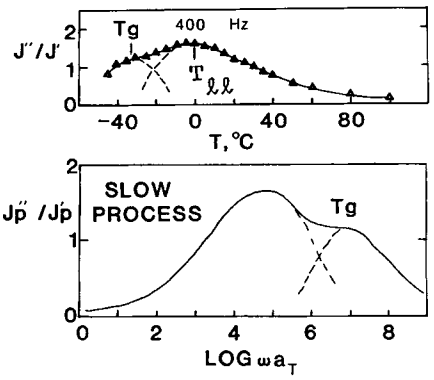

Fig. 8. Dynamic mechanical loss, tan δ = J″/J′, of PIB, $\overline{M}_v$ = 1,350,000 based on data of Fitzgerald et al. A. Adapted from Figure 7 of Ref. 45, at f = 400 Hz. B. Adapted from Figure 5 of Ref. 46. ω is the angular frequency and a_T is the WLF reduction factor. The T_{ll} assignment is ours. This loss peak is called the "slow process" by Ferry and his students.[47]

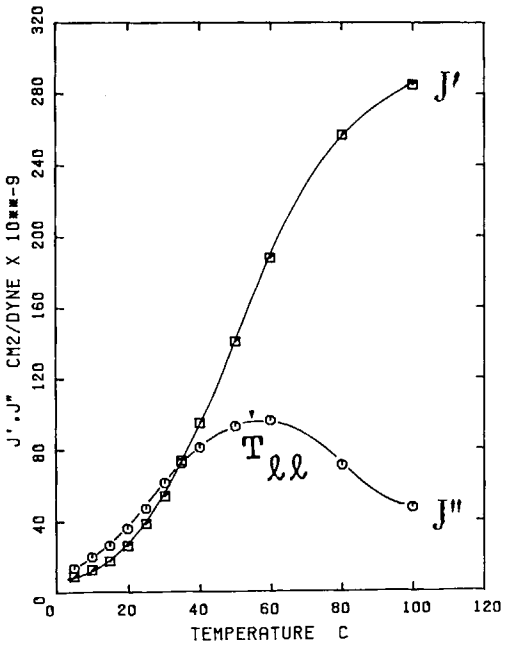

Fig. 9. J'(□), and J'' (○), for PIB for $\overline{M}_v$ = 1,350,000 at 600 Hz from data in Appendix to Ref. 45. T_{ll} assignment is ours. T_g is off scale at circa −40°C. Loss peaks in J'' at 280, 400, and 600 Hz appear as Figure 2 of Ref. 6. (Such plots were not published by the authors of the data in Refs. 45 and 46.)

In our current study which considers the simultaneous existence of T_{ll} and T_{lp}, we naturaly reexamined the J'' vs. T plots for evidence of a double loss peak. Figure 10 shows J'' vs. T plots at six different frequencies. There is a suggestion of a double loss peak at 140 and 200 Hz although one may easily choose to show a single broad maximum. Available J'' vs. T data at 60 and 80 Hz both indicate T_{max} as 30°C. Data above 600 Hz did not exhibit a maximum in J''. Peak widths at half peak height are included in the figure. They increase somewhat with frequency.

3. Stoll et al.[43] used PIB of 4,700,000 viscosity average molecular weight. Their Figure 22 shows J'' as a function of temperature from −130 to 50°C and a frequency range from 10^{-4} to about 10^{7} Hz. It seems certain that several types of apparatus were used even though not specified. They referred to a series of master's theses as source material. It is clear from the relaxation map which they presented in their Figure 19 that the T_g locus as a function of frequency was similar for dielectric loss, ε'', and shear loss modulus, G''. They also showed the locus of a slow process by J'' which agreed with the J'' vs. f data of Ferry et al.[45,46] which they also plotted on their Figure 19.

4. Sanders and Ferry[47] followed mechanical loss in a series of vulcanized butyl rubbers. Plots of log tan δ vs. log a_T showed a T_g peak for all specimens, while a slow process peak was suppressed at higher levels of crosslinking. They ascribe this slow relaxation process to the rearrangement of untrapped

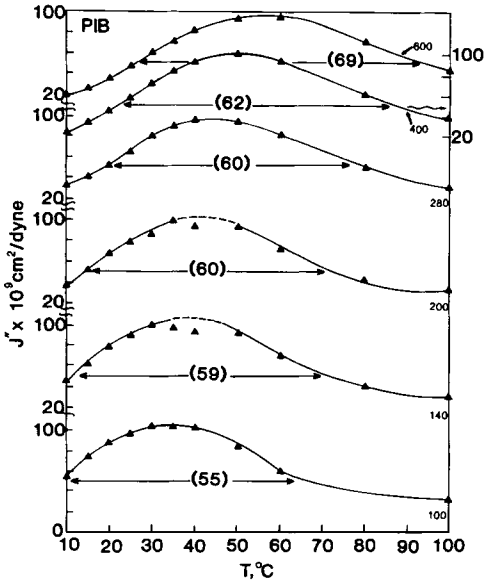

Fig. 10. J″ in units of 10^9 cm^2/dyne at indicated frequencies from Appendix to Ref. 45. Use right hand ordinate for 400 Hz. Numbers in parenthesis are half widths in degrees K at half peak heights. (These data not plotted as such in Refs. 45, 46.)

entanglements of branched dangling structures which of necessity must occur at low degrees of crosslinking.

In a subsequent paper by Valentine and Ferry[48] on polybutadiene (PBD) they observed the slow process even with an unvulcanized specimen so that the presence of mild crosslinking is not a necessary condition for occurrence of the slow process. Of course, the PBD with $\overline{M}_c = 1500$ was highly entangled as was the PIB of Schmieder and Wolf[44] and Fitzgerald et al.[45]

Sanders and Ferry (their Figure 7) also compared intensities of the slow process in several elastometers at similar levels of crosslinking. The slow process is strongest in butyl, weakest in *cis-trans* PBD. This is consistent with the chain stiffness parameters, σ, of these two polymers, i.e., 1.7 and 1.3, respectively.[49] (However, see Table IX of Ref. 38, which emphasizes stereochemical factors.)

5. Kramer et al.[50] blended relatively low-molecular weight PIB with butyl rubber and then vulcanized the system. The slow process loss peak was considered to arise from the free PIB, whose motion within the host network was ascribed to a process of reptation.

6. Wei[51] used TBA to measure six specimens of PIB, all but one of which had $\overline{M}_w > \overline{M}_c$. The lowest molecular weight sample, actually an oligomer, gave clean cut evidence for T_{ll} and $T_{l\rho}$. The results for relatively rigidity and log decrement are illustrated in Figure 11. The values of T_{ll}/T_g given in Figure 11 (1.17) is very similar to the corresponding value for PIB of 4900 molecular weight (1.20) from heat capacity experiments[11], although it represents static values rather than the 0.3 Hz values of Figure 11.

In the other five specimens studied by Wei, with $\overline{M}_n$ values ranging from 7100 to 860,000 and $\overline{M}_w$ from 82,000 to 2,800,000, the transition temperature

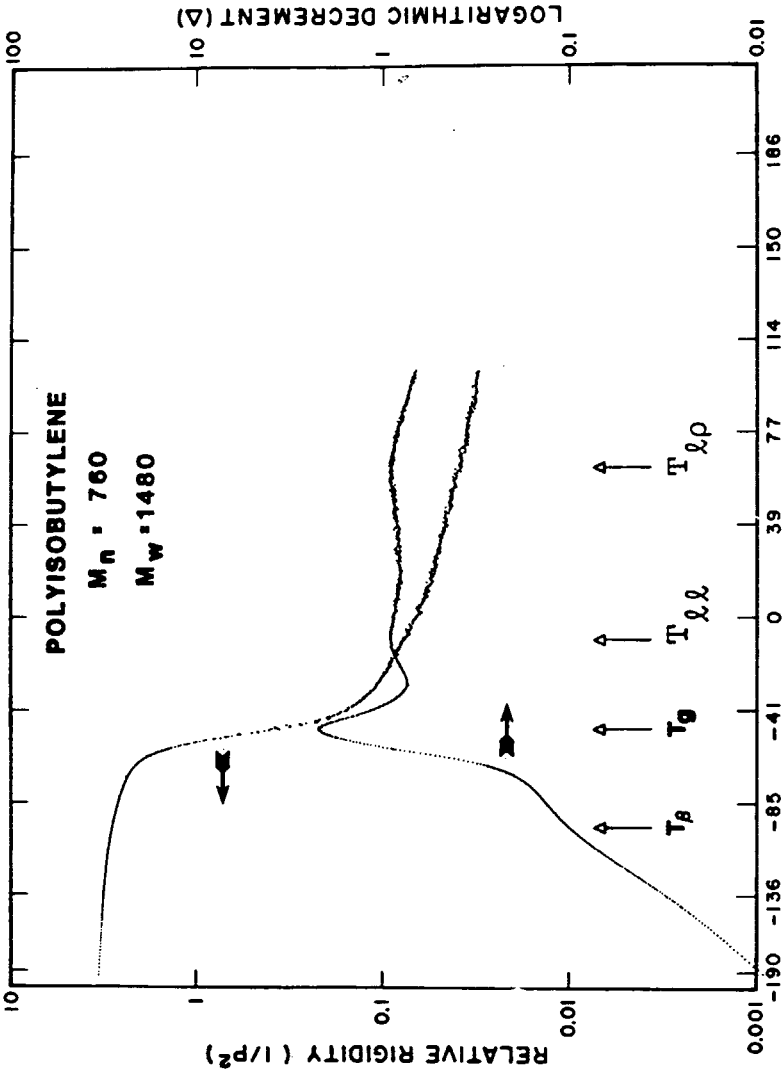

Fig. 11. Log decrement and log relative rigidity for PIB of $\overline{M}_n = 760, \overline{M}_w = 1480$ by torsional braid analysis from the thesis of Wei.[51]

increases rapidly with increasing molecular weight as was found for PS[52], since $\overline{M}_w > \overline{M}_c$. In fact it is off scale (>200°C) for the four highest molecular weight specimens. The peak labeled $T_{l\rho}$ does not appear at all in specimens with $\overline{M}_w$ above $\overline{M}_c$ in Wei's data.

The peak that appears just above T_g as a shoulder in some specimens, and is invariant with $\overline{M}_n$, might represent a viscoelastic interaction between molten polymer and glass braid, of the kind proposed by Nielsen.[53]

7. A more limited study involves use of the DuPont dynamic mechanical analyzer [DMA] 981[28] with the shim stock technique proposed by Starkweather and Giri.[27] A piece of metal or other rigid material about 5 to 10 mil thick and free from mechanical loss over the temperature and frequency range of interest, is used to drive the DMA slave arm at relatively constant frequency. This shim stock is coated on both sides with 5 to 10 mil of the polymer to be studied. Whereas Starkweather and Giri were primarily interested in the T_g region, we have been able to observe mechanical loss behavior at least 100 K above T_g.[28] This study of PIB employed perforated shim stock on four specimens of PIB. Starkweather and Giri[27] emphasize that the shim stock method operates in flexure, thus yielding values of E' and E″. Ideally, there is no shear present as with the Fitzgerald apparatus or TBA.

Three different molecular weight specimens whose characteristics are listed in Table I were studied on heating and cooling with T_{ll} results for heating shown in Table I. $T_{l\rho}$ was not observed, presumably because of greatly increased fluidity above T_{ll}. T_{ll} was most intense in the specimen of lowest molecular weight. This same molecular weight effect on intensity was noted for PS.[52] Since $\overline{M}_w$ varied by a factor of 30, T_{ll} was clearly not influenced by Newtonian viscosity as the mechanism of Nielsen would require.[53] In fact, T_{ll} was clearly leveling off consistent with the absence of shearing effects in the DMA.

Nielsen[53] was concerned with the composite glass braid-polymer specimen used in torsional braid analysis (TBA) where shear is present. The perforated shim stock technique also involves a composite specimen but with totally different geometry and different deformation mode, namely flexure. Figure 12A is a copper shim stock loss curve for PIB.

8. Rheovibron data with filter paper support. Cowie has developed a technique of measuring the viscoelastic behavior of polymers above T_g by impregnating them in filter paper. He kindly agreed to measure the same three specimens measured by the shim stock method. His results are also summarized in Table I. We will return to these data later in connection with Figure 13. Figure 12B shows one of Cowie's runs.

9. Encapsulation with DMA. Encapsulation of one part PIB with 2 to 3 parts of PS in a solvent by codissolving, stirring and freeze drying yielded specimens which could be molded into strips and measured by DMA.[29] The PIB existed as discrete droplets in a continous matrix of PS. While the composite specimen is deformed in flexure, it is acting on the encapsulated PIB. In any event a multiple loss peak for PIB, similar to the one from shim stock, was observed with the following results: $T_\beta = -82$°C; $T_g = -52$°C; and $T_{ll} = -20$°C. In one experiment a minor amount of grafted PS on PIB

TABLE I
T_β,T_g and T_{ll} (K) of PIB vs. Molecular Weight

Specimen		Perforated brass shim stock[b]				Rheovibron[c]			Torsion braid analysis[d]				
$\overline{M}_n$	$\overline{M}_w$	T_β	T_g	T_{ll}	T_{ll}/T_g	T_g	T_{ll}	T_{ll}/T_g	T_β	T_g	T_{ll}	T_{ll}/T_g	$T_{l\rho}$
760	1480	—	—	—	—	—	—	—	179	223	260	1.17	333
7100	81,800	—	229	260	1.14	230	248	1.08	177	216	325	1.50	—
(2814)[a]				(15.6)		(11)	(11)		(≈ 2)	(≈ 1)	(≈ 0.5)		
691,000	2,342,000	—	230	265	1.15	228	248	1.09	178	215	—	—	—
(6085)[a]				(15.4)									
691,000	2,342,000	179[e]	221[e]	263[e]	1.19[e]	—	—	—	—	—	—	—	—
859,000	2,816,000	—	230	263	1.14	230	247	1.07					
(6084)[a]				(14)					180	215	—	—	—

[a] Numbered specimens from Polysciences Laboratory, Specimens supplied by MMI to Prof. Gillham and Prof. Cowie. Characterization parameters from Wei Thesis, Ref. 51.

[b] Data from MMI[28], frequency (Hz) in ( ). Method lacks sensitivity in $T_{l\rho}$ region. T_{ll} also appears on cooling.

[c] Prof. J. M. G. Cowie, University of Sterling, Scotland, unpublished (frequency 11 Hz).

[d] From Wei Thesis, Princeton Univ. Ref. 51.

[e] Measured by Dr. K. Varadarajan, formerly of MMI, using unperforated copper shim stock with DuPont 990-980 DMA used in Ref. 28.

Note: Values of T_g and T_{ll} appear to have leveled off with M which usually happens near the entanglement value, M_e = 17,000 for PIB. The Rheovibron consistently gives low values of T_{ll}/T_g[24.25] as if the applied tension were lowering T_{ll}.

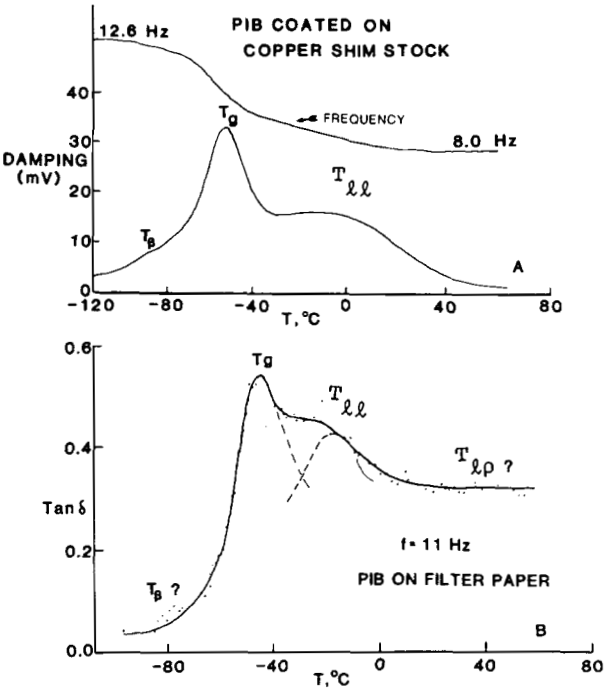

Fig. 12. A: Dynamic mechanical loss of PIB, $\overline{M}_n$ = 691,000 on unperforated copper shim stock using the DuPont 990-980 DMA method. Resonant frequencies are shown at top, loss (G'') in millivolts at bottom. Heating cycle. See Table I for other details. Method described in Ref. 28. B: Dynamic mechanical loss of same PIB from Rheovibron at 11 Hz, with specimen impregnated into filter paper. Data of Cowie.[26]

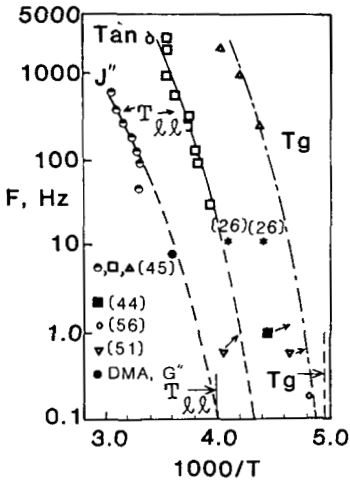

Fig. 13. Low frequency relaxation map for PIB based on T of J'_{max} from Figure 9 and tan δ_{max} calculated from data in Appendix of Ref. 45. Additional values of T_g and T_{ll} from Table I are indicated. See Figure 15 for a high frequency relaxation map.

was used as a polymeric emulsifier to aid in the dispersion of PIB in PS. The results were essentially the same.

We can summarize this section by noting that one, or in some cases, two dynamic mechanical loss peaks above T_g have been observed by several different methods:

1. The hanging torsion pendulum in angular shear;[36]
2. The Fitzgerald apparatus in vibrational shear;[37–40,45]
3. Torsional braid analysis which applies angular shear to a composite specimen; glass braid impregnated with molten polymer.[41]
4. DMA–981 which applies flexure to the shim stock[42] and to the encapsulation.[43]
5. The Rheovibron in tension.

Yet all give roughly comparable results, when the molecular weight, frequency and the function being plotted: (E'', J'', $\pi \tan \delta$ = log decrement) are taken into account. Moreover, these dynamic mechanical results are compatible with results from nonviscoelastic methods such as C_p, DSC, P–V–T, and ^{13}C NMR. Considering all of the examples just cited, it follows that PIB oligomers and polymers have been observed in the liquid state well above T_g in two general cases:

I. Unsupported specimens
  A. Highly entangled specimen, $M >> \overline{M}_c$.
  B. Lightly vulcanized specimens
II. Mechanically supported specimens
  A. TBA
  B. Polyblends (PIB in vulcanized butyl)
  C. Shim stock
  D. Encapsulation (low modulus PIB in High modulus PS)

The important elements appear to be one or more of the following:

1. Minimization of creep by using physical entanglements or vulcanization
2. Mechanical support of the pendulum in TBA
3. Maintaining modulus above T_g to drive the apparatus, as with DMA and the shim stock or the encapsulated specimen.

We conclude this section on dynamic mechanical analysis by discussing the frequency dependence of T_g and T_{ll}.

A LOW FREQUENCY RELAXATION MAP

In an earlier study[6] we presented a log f vs. $1/T$ relaxation map for T_g and T_{ll} based primarily on the low frequency data from Fitzgerald et al.[45] with a few additional data points. Meanwhile the data analysis techniques have been refined and new results have been obtained. Figure 13 is an updated version of Figure 4 in Ref. 6. It shows T_g and T_{ll} by two methods:

T_{max} for J″ from Figure 9 and T_{max} for tan δ from plots not shown but prepared from the J′ and J″ data in Ref. 45. Static values for T_g from the literature (circa 202 K) and for T_{ll} from the C_p data in Figure 3 are indicated. We consider the J″ line for T_{ll} to be the correct one. It is the locus shown in figure 10.24 of McCrum et al.[54] but incorrectly considered by them to represent T_g, as well as the line labeled B in Figure 19 of Stoll et al.[43] which is a composite of their newer T > T_g data with the data from Ref. 45. Both Refs. 43 and 54 show points from J''_{max} at lower frequencies than are possible from the tabulated data in Ref. 45, i.e., below 1 Hz, and must have been obtained by some extrapolation procedure.

It is proper that the T_{ll} line from tan δ be at lower temperatures than for J″ since tan δ is obtained by dividing J″ with J′ which is a rapidly increasing function of temperature, as seen in Figure 9. We have discussed in connection with Table 1 of Ref. 7 the opposite shift which results when tan δ is calculated from G''/G'.

Figure 13 contains data points at 15 Hz from the shim stock method and 11 Hz from the Rheovibron method both in Table I. We average in each case for the three molecular weights since all are on the T_{ll} plateau. The shim stock value of T_{ll} falls on the J″ line, confirming what Starkweather had told us.[55]

The Rheovibron point at 11 Hz shows T_g as being essentially correct but T_{ll} being low (as evident from Table I) but close to the tan δ line.

The TBA T_g point of Martin and Gillham[56] is correct but they did not list a T_{ll} value because their temperature range was insufficient. The TBA points for Wei and Gillham[51] (with $\overline{M}_n$ = 8100, $\overline{M}_w$ = 81,800) are also shown.

We finally consider one other aspect of the log f vs. $1/T$ curve from J″. The plots of log f vs. $1/T_{max}$ where the temperature is that of the maximum in J″ vs. T are curved concave downward. This is evident in the high temperature process of figure 10.41, Ref. 54; Figure 20 of Ref. 10 and Figure 4 of Ref. 6. It is further confirmed by Figure 19 of Ref. 43 in which the Ferry et al. and the Stoll et al. data are compared. Hence log f vs. $1/T$ does not obey simple Arrhenius behavior but appears to follow a Vogel–WLF type of equation

$$f = A \exp [-B/(T - T_0)] \tag{4}$$

We have now determined by trial and error that T_0 is 265 K. This is the asymptotic limit approached at low frequency and should correspond closely toT_{ll} from C_p, as it does. The curved plot extrapolated on either side by Eq. (4) will appear on the relaxation map given later as Figure 15, the high frequency relaxation map, which emphasizes still other features.

ZERO SHEAR MELT VISCOSITY

An earlier study[5] reviewed several sets of log η_0 vs. $1/T$ data for possible evidence of T_{ll}. (η_0 is zero shear viscosity.) Slope changes were indeed found and cited as indicative of T_{ll} even though some of them tended to be higher in temperature than expected. The most convincing data set was that of Ferry and Parks[57] on the same PIB specimen (M = 4900) for which C_p data

were available as shown in Figure 4. An intersection in the log η_0 vs. $1/T$ plot occurred around 258 to 260 K.

More recently we have examined by regression analysis an extensive set of zero shear viscosity data on PS's with $\overline{M}_w/\overline{M}_n \approx 1.1$ covering a broad range of $\overline{M}_n$ and a wide range of temperature.[15] This data clearly showed evidence for both T_{ll} and $T_{l\rho}$. Such extensive data are not available for PIB.

Reexamination of the Ferry and Parks data by improved regression analysis techniques has produced the results shown in Figure 14. It is the RES/SE $\hat{Y}$ plot of a linear fit of the η_0 vs. $1/T$ values. It is clearly nonrandom and indeed shows evidence of a double break similar to that seen in Figure 4 by C_p. There are only three points defining the middle line. However, we feel justified in indicating both T_{ll} and $T_{l\rho}$ in view of Figure 4.

Intersection temperatures reported earlier[5] for the Ferry et al. data occurred at 307 to 309 K; for the Fox and Flory data: 290 K at M = 80,000, 318 K at M = 600,000. Since $M > \overline{M}_c$, this could be a result of entanglements, especially if true zero shear conditions did not prevail.

The reassignment of these various data sets in comparison with the view presented earlier[5] results from experience with PS,[15] improved regression analysis techniques, and more familiarity with $T_{l\rho}$ data.

A RELAXATION MAP FOR PIB

The conventional low frequency relaxation map shown earlier as Figure 13 seemed adequate for discussion of T_{ll} when we first prepared it.[6] However, we were not then aware of the relaxation map by Stoll et al., rather lost in a publication on the bundle model.[43] It not only confirmed Fitzgerald et al.,[45] but showed the first locus for a β process at $0.75T_g$. Then the importance of very high frequency data on T_g became apparent from studies by Törmälä[22] as well as by Lobanov and Frenkel,[23] also confirmed by Stoll et al.[43] It therefore seemed pertinent to prepare a high frequency relaxation map specific to the topic of T_{ll}. We start with a sequential review of PIB maps.

Various maps of log f vs. $1/T$ have appeared from time to time, each differing somewhat according to the interests of the author, and/or accessible data.

The earliest relaxation map known to us is that of Thurn[39] (Hendus et al.[59]) and is actually in the form of a log f vs. T(°C) plot. It contains a considerable amount of diverse types of data from dynamic mechanical to NMR to ultrasonics, covering the frequency range from 10^{-1} to 10^7 Hz. It shows the locus for CH_3—group rotation from NMR for the first time.

This map shows the locus of a relaxation lying above T_g with an activation enthalpy, ΔH_a, of 19 kcal/mol compared to a value of 38 kcal/mol for T_g. This line, which we ascribe to T_{ll}, confirmed a low frequency loss tendency for ΔH_a at T_{ll} to be about half of ΔH_a at T_g. Thurn's map seems clearly the first to show a locus for T_{ll} in PIB.

Slichter then presented a relatively simple relaxation map[60] giving the locus for T_g by mechanical, dielectric and NMR and for CH_3—group motion by NMR. He credited this map to McCall. Next was that of McCrum et al., Figure 10.24 of Ref. 54, combining mechanical and dielectric loss data to show T_g. As already noted, a $T > T_g$ line based on the J″ data of Fitzgerald

et al. was incorrectly ascribed to T_g but is indeed T_{ll}. McCall[61] provided twelve literature citations including the ultrasonic loss data of Thurn and detailed references to NMR data. He showed only the T_g line by mechanical, dielectric, and NMR data, and the δ or CH_3–line by NMR.

The next map to appear was that of Stoll et al.[43] Their Figure 19 combined new dielectric and mechanical loss data of their own (already cited) with literature results. They show three $T < T_g$ loci, labeled γ,γ′ and δ, the latter at the lower temperature. γ′ is near δ and may be the mechanical loss for CH_3–rotation defined by the δ NMR line. The line labeled γ is closer to the T_g line and eventually intersects it. We suggest that this is the $T < T_g$ or T_β relaxation process, this being its first appearance in the literature. Figure 11, shown earlier, clearly shows such a loss peak. Its location at 179 K at a frequency of 1 Hz falls very close to the γ line. Moreover, this γ line clearly joins up with the T_g line around 10^5 to 10^6 Hz. Their T_g line, labeled β′, is based on their own dielectric and mechanical loss results. We prefer to label it as T_g.

Another locus, labeled $\beta > T_g$, plots the combined J″ loss data of Ferry et al., shown earlier in Figure 9, with their own J″ results. This is what we label T_{ll}. The agreement between the two sets of dynamic mechanical J''_{max} data is excellent. The Stoll et al. specimen had a molecular weight greater than 4,000,000. Thus the Stoll et al. data confirms the 1953 conclusion of Fitzgerald et al.[37] that their $T > T_g$ loss peak was not an artifact.

The most recent relaxation map we have is that of Törmälä, Figure 17 of Ref. 22, with particular emphasis on ESR spin probe data. The γ, γ′ and δ data of Ref. 43 is shown, but not the $T > T_g$ locus.

Finally, we direct attention to the relaxation maps of Lobanov and Frenkel[23] consisting of log τ vs. $1/T$ plots with heavy emphasis on dielectric loss data, where τ is the relaxation time. They ascribe special significance to the kink in the T_g locus, labeled T*, which occurs near where the locus of $T < T_g$ line appears to join the T_g line. This latter point is also made by Törmälä 22, and indeed by various authors such as Mikhailov et al.[62] Patterson stated that a single loss datum from Brillouin scattering in PIB at the hypersonic frequency of circa 10^{10} Hz fell on an extension of the $T < T_g$ locus above where it merged with T_g.[63]

Lobanov and Frenkel[23] deduced from an examination of extensive dielectric and other literature data the relationship

$$T^* = T_g + 76\text{K} \tag{5}$$

where T_g is the static value of the glass transition temperature. They concluded that T* constitutes evidence for T_{ll}. They did not present a log τ vs. $1/T$ plot for PIB but Törmälä did in Figure 17 of Ref. 22. However, the kink is not especially pronounced because of heavy emphasis on ESR data at high frequency.

None of the above-mentioned sources included the acoustic attenuation data on PIB by Ivey et al.[36,37] We had long been aware of this high frequency loss data but its relevance to T_{ll} did not become apparent until the Lobanov–Frenkel concept appeared. The points shown represent the temperatures of maximum attenuation in decibels per cm.

Having in mind the background material just cited, we now construct a relaxation map for PIB pertinent to the present inquiry, as shown in Figure 15. The T_g line to 10^4 Hz is taken from McCall;[52] data points in the kink region and above are from Ivey et al.;[55] the hypersonic data point based on Brillouin scattering is from Patterson.[63] The T* value is well defined at a temperature of 260 K, and hence very close to the T_{ll} value of 252 K in Figure 4. This certainly appears to confirm the concept of Lobanov and Frenkel[23] as expressed by Eq. (5).

The locus labeled T_{ll} is based on the J″ vs. T data plotted in Figure 10 and the J''_{max} vs. $1/(T - T_0)$ plot (not shown) at low frequencies, from which the dotted extensions were calculated. This locus is shown approaching the asymptotic limit of T_{ll} = 252 K from C_p data in Figure 3. This may well represent a merged $T_{ll} - T_{l\rho}$ locus. The high frequency values of T_{ll} are from the ultrasonic loss points originally collected by Thurn[39] and Hendus et al.[59] Since they were estimated from plots, they show scatter. They seem to fall on the tan δ line for T_{ll}.

The γ line of Stoll et al. which we would label T_β is close to the slope of the high frequency part of the plot.

We consider this map fully consistent with the concept of T_{ll} both from the kink in the T_g plot occurring at T* and from the extrapolation of the T_{ll} data from J″ to the asymptotic low frequency value from C_p data.

We suggest that Figure 15 constitutes the most complete and best documented relaxation map for PIB yet published, particularly in conjunction with Figure 13.

DISCUSSION AND RESULTS

It seems clear from the material presented herein that there is ample evidence to support the existence of a strong T_{ll} in PIB and butyl rubber by both relaxational and quasistatic or thermodynamic data. The same has long been known for T_g. There is less evidence to suggest a $T_{l\rho}$ process lying above T_{ll}. Table II summarizes results by the various quasistatic methods. One may question log η_0 as being a quasistatic method but we reached this conclusion in a similar study on PS.[15] It appears that the true zero shear state, even when obtained by extrapolation, represents a nonflow test.

One gratifying result of this study is the showing of consistent 3 line RES/SE $\hat{Y}$ patterns for two sets of C_p vs. T data (Figs. 3 and 4), isothermal V vs. P data (Fig 7), and log η_0 vs. $1/T$ data (Fig. 14) all indicating T_{ll} and $T_{l\rho}$ with a remarkably narrow range of temperature values as listed in Table II.

We had long been concerned that frequency dependent $T > T_g$ loss peaks on PIB first reported by Fitzgerald et al.[45] did not appear to have been verified. Fortunately, this was an incorrect conclusion. Location of the 1972 relaxation map by Stoll et al.[43] provided not only this much needed verification of T_{ll} by J″ but also dielectric loss data at T_g and possibly at T_{ll}, and the β relaxation at about 0.75 T_g hitherto observed only by TBA.[51] Finally, Table I presented evidence for T_{ll} by three other dynamic mechanical loss techniques.

TABLE II
Summary of T_{ll} and $T_{l\rho}$ (K) Values Quasi-equilibrium Data (No Flow)

Method	Mol. wt.	T_g	T_{ll}	T_{ll}/T_g	$T_{l\rho}$	$T_{l\rho}/T_g$	Source
Specific Heat, C_p	$\overline{M}_v$ = 1,350,000	200(3)	253	1.27	292	1.46	Figure 3
Specific Heat, C_p	4900	197(11)	236	1.20	266	1.35	Figure 4
Thermal diffusivity,α[a]		—	253	—	—	—	(Ref. 32)
DSC (10 K/min)	$\overline{M}_n$ = 7100	209	246	1.18	—	—	Figure 5
Ultrasonic velocity,ν_s (10MHz)[b]	Vulcanized butyl gum stock	200	250	1.24	282	1.40	Figure 6
^{13}CNMR		203	263	1.30	—	—	(Ref. 13,42)
Collapse Temp., T_c							
T*[c]	Various	200	263	1.32	—	—	Figure 15
Zero shear melt viscosity, η_0	4900	197	241	1.22	263	1.34	Figure 14
Isothermal V-P (84.8°C)	36,000	200	808 *bars*[d]	—	538 *bars*[d]	—	Figure 7
T_0 of Vogel Eq. (4)	1,350,000	200	265	1.33	—	—	Eq. (4)

[a] Thermal diffusivity, $\alpha = \lambda/\rho C_p$ where λ is thermal conductivity, ρ is density and C_p is specific heat. Ueberreiter employs an instrument which measures it directly.[32]

[b] T_g at 10 MHz is at 313 K (See Figure 15).

[c] This is the Lobanov-Frenkel temperature[23] at which there is a sharp slope change at about 10^6 Hz in log f vs. $1/T_g$ plots, as illustrated in Figure 15.

[d] Extrapolation to P = 1 of such pressures for a series of isotherms gives T_{ll} and $T_{l\rho}$ comparable to the other values as was shown for PIB in Ref. 14.

Note: See Appendix I for dependence of T_g and T_{ll} on $\overline{M}_n$ and $\overline{M}_w$.

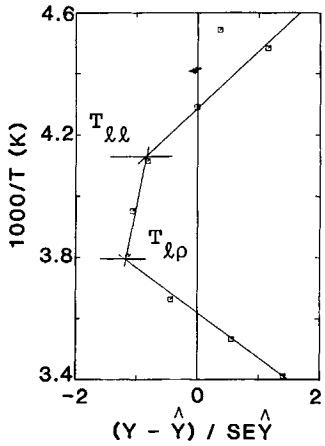

Fig. 14. RES/SE $\hat{Y}$ pattern for a linear fit to the log zero shear melt viscosity (η_0 vs. $1/T$) data of Ferry and Parks[57] on PIB of M = 4900. T_{ll} and $T_{l\rho}$ values are shown. Methodology for such plots is given in Ref. 15, where it is shown that while melt visosity data is dynamic, results appear to give static values of T_{ll} and $T_{l\rho}$ as listed in Table II.

Comparison in Table I between several dynamic mechanical analysis techniques is quite good although they differ in support medium and mode of deformation. Frequency dependence was to be expected. Consistency between T_{ll} values for the unsupported data of Ref. 45 and some of the supported results in Table I appear in Figure 13.

T_{ll} in PIB is relatively strong compared to its value in other polymers. Sanders and Ferry[66] compared the intensity of their slow process ($\equiv T_{ll}$ in our view) for five common elastomers. Intensity of the mechanical loss peak was greatest for butyl rubber, lowest in *cis-trans*-vinyl PBD.

While PIB is essentially nonpolar, it does possess a relatively stiff chain which is one of Frenkel's requirements for a strong segment–segment interaction. Moreover, PIB has a simple head to tail structure free of steric imperfections. Packing must be good—just short of that needed for crystallinity since it does crystallize readily on stretching. Evidence for structure in PIB has been found by Stevens and Roe using the positron annihilation technique.[67] They note that packing in the more ordered regions, which is decreasing with temperature, appears to have reached an equilibrium above -25°C ($T_{ll} = -20$°C).

There has been a trend especially with PS, to downgrade T_{ll} as a purely relaxational event with no basis in thermodynamics[68,69] or to dismiss it completely as an artifact of the test method.[70,71] We respond herein to the first point by emphasizing both the relaxational and the quasiequilibrium evidence for T_{ll} (Table I). We respond to the artifact issue by emphazing the multiplicity of relaxation and quasiequilibrium methods yielding comparable values of T_{ll}. We consider that while one or several methods may be suspect, it is highly improbable that they all are.

While there is no question about a definitional distinction between a transition and a relaxation,[69,72] the differences may be blurred in regard to experimental results. The ^{13}C NMR collapse temperature, T_c, at a nominal frequency of 10^3 to 10^4 Hz agrees, for PIB, with the static value of T_{ll}.[13]

The use of ultrasonic velocity data in Figure 6 to locate T_{ll}, which agrees with T_{ll} by C_p, is an ideal illustration of our point. If the dispersion region for T_g is at a sufficiently high temperature, the bulk velocity wave responds to the static drop in density at T_{ll}.

The relaxational-transitional nature of T_g and T_{ll} is also evident in Figure 15. T* from mechanical or dielectric or NMR data for T_g, and T_o from dynamic mechanical loss data both derive from relaxational data and yet agree with quasistatic C_p data. T_{ll} determined directly from J″ in Refs. 43 and 45 follows a WLF type of behavior and responds to free volume changes.

Lobanov and Frenkel (pages 1159–60 of Ref. 23) are explicit in stating that T*, while obtained from a relaxational method, should not be construed as being purely relaxational in character. They emphasize that a relaxation event would change slope gradually as free volume increases, in constrast to the sharp slope change at T* in Figure 15.

Finally, we note that the ESR spin probe technique, although not yet demonstrated in PIB, located T_{ll} in PS and in PP at 1.15 T_g with a sudden change in the sharpness of the spectra.[64,65]

SUMMARY AND CONCLUSION

We start by demonstrating with objective statistical computer techniques that C_p vs. T data above T_g for a PIB of $\overline{M}_v$ = 1,350,000, long claimed to

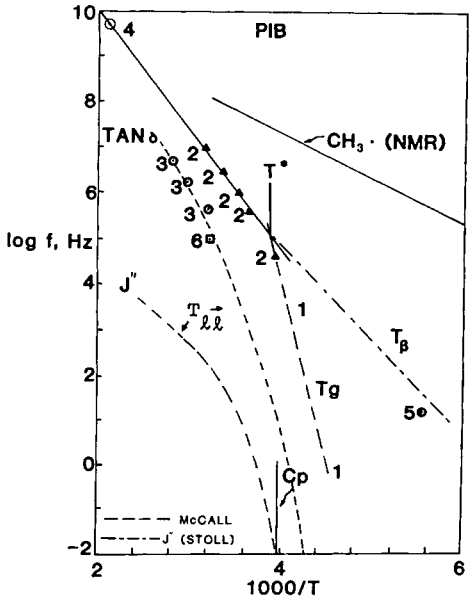

Fig. 15. General Relaxation map for PIB or butyl rubber with special emphasis on high frequency data for T_g, T_{ll}, and T_β. Sources of data are as follows: (1) Mechanical, dielectric and NMR plots from Slichter[60] and McCall[61]; (2) Ultrasonic attenuation in db/cm for vulcanized butyl rubber gum stock from Ivey et al.;[36,37] (3) Ultrasonic loss for T_{ll} from Figure 2 of Thurn[39] or Figure 26 of Hendus et al.;[59] (4) Brillouin scattering of Patterson,[63] T_β line from Stoll et al.;[43] (5) DMA from Table I for T_β; (6) NMR, Thurn.[39] Vertical line labeled C_p is T_{ll} from Figure 3. Vertical line labeled T* locates T_{ll} by the method of Lobanov and Frenkel[33] and is shown for the first time for PIB. The T_{ll} line below 10 kHz is from J″ data of Figure 13; above 10 kHz as indicated.

follow a quadratic, acquired that quadratic character because of a smooth curve hand drawn through the raw data. Computer analysis of the raw data revealed three straight line segments whose intersections were labeled as the liquid–liquid transition (relaxation), T_{ll}, at 253 K and a $T_{l\rho}$ process at 290 K. A second set of C_p vs. T data for PIB (M = 4900) by different authors also showed these same two events, each at a lower temperature.

We then proceeded on the hypothesis that if our statistical procedure was correct in locating molecular level events, T_{ll} and possibly $T_{l\rho}$ should be revealed by a large variety of quasistatic and relaxational methods, some of which were already known to us through earlier studies.[5,6] Our goal was to present a definitive review of T_{ll} from the open PIB literature, some of which was so old that it had been forgotten and some of which was buried in obscure places because of faulty abstracting.

Quasistatic results are summarized in Table II. Older dynamic mechanical and other relaxational data are summarized by relaxation maps in Figures 13 and 15 while newer dynamic mechanical loss data are given in Table I.

We demonstrate for the first time in Figure 6 that T_{ll} and $T_{l\rho}$ are observed in ultrasonic velocity data at 10 MHz. We further show for the first time in Figure 15 the T^* temperature of Lobanov and Frenkel for PIB and demonstrate that while T* derives from relaxational type data, yet $T^* = T_{ll}$ from quasistatic C_p data, consistent with the generalized prediction of Lobanov and Frenkel for all polymers.[23] We note that the molecular weight dependence of T_g and T_{ll} are weak compared to those for PS and PMMA. Lastly, we note the relationship between the strong T_{ll} in PIB and Butyl and the unusually low resiliency of butyl at ambient temperatures.

APPENDIX I

Molecular Weight Dependence of T_g and T_{ll}

The prediction of a molecular weight dependent $T > T_g$ was made by Ueberreiter as early as 1943[73] based on his concept that T_g occurs when intermolecular forces are surmounted and intramolecular barriers require a higher temperature which he labeled T_f. T_f and T_g are shown as identical for oligomers but as T_g levels off T_g and with increasing molecular weight, T_f starts to increase without limit. Ueberreiter considered that in the region between T_g and T_f the polymer was superficially a liquid but one with fixed structure. In his view the true liquid state occurs only above T_f.

The first experimental verification of Ueberreiter's views are provided by the penetrometer data of Kargin and Sogolova.[74–76] They referred to their $T > T_g$ event as T_f but made no reference to the earlier paper by Ueberreiter. They characterized specimens by dilute solution viscosity but then converted to molecular weights by two different sets of Mark–Houwink constants. Figure 16 is a plot of T_g and T_f against log $\overline{M}_v$ using the relationship

$$\eta_{sp} = 1.75 \times 10^4 CM \qquad \text{(AI-1)}$$

where η_{sp} is the specific viscosity, C is in base moles per liter, and M is molecular weight. This is Staudinger's law. We chose Eq. (6) because the sharp upturn in T_f occurs just above $\overline{M}_c$, the entanglement molecular weight,

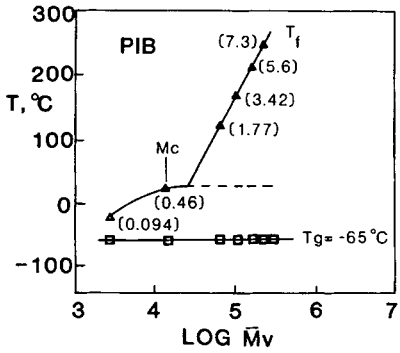

Fig. 16. T_g and T_f by the method of penetrometry based on data of Kargin and Sogolova.[74] Bottom scale, Staudinger molecular weights with vertical bar at $\overline{M}_c$ = 17,000. Dashed line, T_{ll} above $\overline{M}_c$ by nonmelt flow methods. Numbers in parentheses are intrinsic viscosities. This plot contains the first experimental evidence for T > T_g in any polymer.

which is about 17,000.[77] This arbitrary procedure is based on a showing by Ueberreiter and Orthmann[78] of a similar upturn in T_f by a different method for fractions of PS and PMMA. There was no question that the upturn occurred at $\overline{M}_c$ = 35,000 for both polymers.

Figure 16 did not appear in the original publication.[74] T_g is essentially flat, agreeing with our demonstration that low T_g polymers have minimal dependence on molecular weight.[79] This was also evident in Table II which showed T_g by C_p increasing only 3 K as molecular weight increases from 4900 to 1,350,000.

Figure 16 shows the typical course for $T_f > T_g$ by a method involving melt flow, as we have demonstrated by the analysis of considerable literature data (see Figure 5 and related discussion in Ref. 10). If however, a nonflow method is used, as with specific heat, T_f will follow the dotted horizontal line in Figure 16. For example, T_{ll} by C_p has leveled off between M = 4900 and M = 1,350,000 to a limiting value of −20°C (see Table II).

In Table I T_g is shown to be independent of $\overline{M}_n$ or $\overline{M}_w$ by all three dynamic mechanical methods. T_{ll} also appears to be independent of molecular weight as if it were following the dashed horizontal line of Figure 16. We expected this for the DMA and the Rheovibron which operate in bending and tension respectively. It was unexpected with TBA.

We note from Figure 13 that the vibrating shear data of the Fitzgerald apparatus[45] gives an asymptotic value of T_{ll} for $\overline{M}_v$ = 1,350,000 which does not reflect the entanglement effect observed for the upper T_g branch of Figure 16.

Finally, we remark that Figure 16 supersedes an earlier attempt to provide a similar map.[5] The general shape was correct but some of the data points were questionable then and now considered incorrect.

APPENDIX II

The Resiliency of Butyl Rubber

According to a series of rebound-temperature plots published by Treloar[80] for common elastomers, the rebound of butyl rubber is abnormal in three

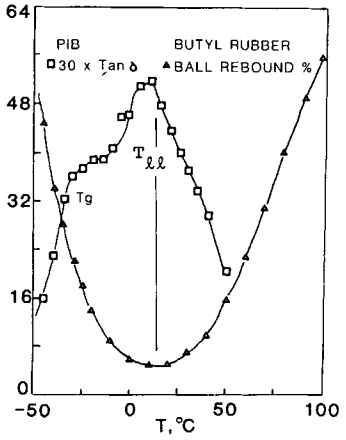

Fig. 17. Tan δ × 30 at 1000 Hz for PIB from Ref. 45. Ball rebound (%) for filled butyl rubber from Ref. 83.

respects: The minimum is very low, very broad and at a temperature high compared with its T_g. The minimum is normally considered to occur at T_g of the elastomer for the effective frequency of the test, normally about 10^3 Hz.[81] T_g should therefore occur at -30°C, because the rebound minimum occurs near 10°C.

Figure 17 was prepared[6] to suggest that the minimum in rebound appears to be associated with the strong $T > T_g$ process in PIB, possibly now with the combined $T_{ll} - T_{l\rho}$ events shown earlier. Alternately, one may state that the presence of such a strong minimum so far above the expected T_g constitutes prima facia evidence for the existence of a strong $T > T_g$ dynamic mechanical loss peak. Since no mechanical support (substrate) is needed in a rebound test, the question of an artifact should not arise. For further details on resiliency in butyl consult Kramer et al.[50] or Kramer and Ferry.[82]

APPENDIX III

Since this manuscript was completed, Maxwell has announced a significant finding about T_{ll} in atactic PS, poly(paramethylstyrene) and atactic PMMA.[84,85] A small but distinct drop in absolute modulus is observed in the T_{ll} region. The temperature at which it occurs increases with molecular weight. This decrease in modulus was apparent but small in the PS relative rigidity data of Stadnicki et al.[52] by the torsional braid method. It accompanied the T_{ll} loss peak, as it should. Maxwell's methods employ pure polymer melts and thus avoid the artifact charge unjustly leveled against the TBA method for the T_{ll} region.[70,71a] Maxwell has not yet studied PIB.

We thank Prof. J. M. G. Cowie for the Rheovibron data of Figure 12B and Table I; the Library of Notre Dame University for access to the Ivey Thesis;[37] Prof. John D. Ferry for correspondence concerning the PIB data from Ref. 45; Prof. K. Ueberreiter concerning his thermal diffusivity studies on PIB; Professor Bryce Maxwell, Princeton University, for placing at our disposal his extensive data on modulus decrease at T_{ll} (mostly on PS) as mentioned in Appendix III; Dr. Richard Pethrick, University of Strathclyde concerning ultrasonic velocity in polymers above

T_g; Mr. Andrew Olah of MMI on the same subject; Mrs. Kathleen Panichella of MMI for the DSC trace of Figure 5, the computer studies and the art work; Prof. John K. Gillham of Princeton University for a detailed reading of the manuscript and numerous helpful comments; MMI Librarians Mrs. Julia Lee and Mrs. Jean Schwind for literature help; and Mrs. Susan Haywood for the electronic typing.

References

1. R. F. Boyer, R. L. Miller, and C. N. Park, *J. Appl. Polm. Sci.*, **27**, 1565 (1982).
2. P. S. Wilson and R. Simha, *Macromolecules*, **6**, 902 (1973).
3. G. J. Furakawa and M. L. Reilly, *J. Res. Natl. Bureau Stds.*, **56**, 285 (1953).
4. R. F. Boyer, in *Thermal Analysis*, (Proc. Third ICTA, Davos, 1971), H. G. Wiedemann, Ed. Vol. 3, Birkhauser, Verlag, Basel-Stuttgart, 1972, pp. 3–18.
5. J. B. Enns and R. F. Boyer, *Organic Coatings and Plastics Chemistry Preprints*, Am. Chem. Soc., **38(1)**, 387 (1978).
6. R. B. Boyer and J. K. Gillham, *Organic Coatings and Plastics Chemistry Preprints*, Am. Chem. Soc., **41**, 430 (1979).
7. J. K. Gillham and R. F. Boyer, *J. Macromol. Sci., Phys.*, **B-13**, 497 (1977).
8. J. K. Gillham, *Polym. Eng. Sci.*, **19**, 749 (1979).
9. R. F. Boyer, *Polym. Eng. Sci.*, **19**, 732 (1979).
10. R. F. Boyer, *J. Macromol. Sci., Phys.*, **B-18**, 461 (1980), esp. 506–11 on PIB.
11. J. D. Ferry and G. S. Parks, *J. Chem. Phys.*, **4**, 70 (1936).
12. K. Solc, S. E. Keinath, and R. F. Boyer, *Macromolecules*, **16**, 1645 (1983).
13. R. F. Boyer, J. P. Heeschen, and J. K. Gillham, *J. Polym. Sci., Polym. Phys. Ed.*, **19**, 13 (1981).
14. R. F. Boyer, *Macromolecules*, **14**, 376 (1981).
15. R. F. Boyer, *European Polym. J.*, **17**, 661 (1981).
16. R. F. Boyer, *Colloid Polym. Sci.*, **258**, 760 (1980).
17. R. F. Boyer, *Macromolecules*, **15**, 774 (1982).
18. R. F. Boyer, *Macromolecules*, **15**, 1498 (1982).
19. J. Grandjean, H. Sillescu, and B. Willenberg, *Makromol. Chem.*, **178**, 1445 (1977).
20. B. Willenberg and H. Sillescu, *Makromol. Chem.*, **178**, 2412 (1977).
21. P. Lindner, E. Rossler and H. Sillescu, *Makromol. Chem.*, **18**, 3653 (1981).
22. P. Törmälä, *J. Macromol. Sci., Rev. Macromol. Chem.*, **C-17**, 297 (1979).
23. A. M. Lobanov and S. Ya. Frenkel, *Polymer Sci. USSR*, **22**, 1150 (1980) translated from *Vysokolmol. Soyed.*, **A-22**, 1045 (1980).
24. a. J. M. G. Cowie and I. J. McEwen, *Polymer*, **20**, 719 (1979); b. *Polym. Eng. Sci.*, **19**, 709 (1979).
25. J. M. G. Cowie, D. Lath, and I. J. McEwen, *Macromolecules*, **12**, 56 (1979).
26. J. M. G. Cowie, Univ. of Sterling, Scotland, unpublished observations on PIB, (1983).
27. H. W. Starkweather and M. R. Giri, *J. Appl. Polym. Sci.*, **27**, 1243 (1982).
28. S. E. Keinath and R. F. Boyer, *J. Appl. Polym. Sci.*, **28**, 2105 (1983).
29. K. Varadarajan and R. F. Boyer, *Organic Coatings and Plastics Chemistry Preprints*, Am. Chem. Soc., **44**, 409 (1981).
30. F. J. Anscombe and J. W. Tukey, "The Examination and Analysis of Residuals," *Technometrics*, **5**, 141 (1963).
31. R. F. Gunst and R. L. Mason, *Regression Analysis and Its Application*, Marcel Dekker, New York, 1980.
32. K. Ueberreiter, in *Plasticization and Plasticizer Processes*, N. J. Platzer, Ed. Advances in Chemistry Series No. 48, Am. Chem. Soc., Washington, D.C., 1965, p. 35ff.
33. L. R. Denny, K. M. Panichella, and R. F. Boyer, *J. Poly. Sci., Polym. Symp.*, **71**, 39 (1984).
34. N. Bekkedehl, *J. Res. Natl. Bureau Stds.*, **43**, 145 (1949).
35. N. Work, *J. Appl. Physics*, **27**, 69 (1956).
36. D. G. Ivey, B. A. Mrowca, and E. Guth, *J. Appl. Physics*, **20**, 486 (1949).
37. D. G. Ivey, *Propagation of Ultrasonic Bulk Waves in High Polymers*, a dissertation submitted to the graduated School of the University of Notre Dame, March 1949.
38. R. F. Boyer, *Polymer Yearbook*, vol. 2, R. A. Pethrick, Ed., Harwood Academic Publisher, London, 1985, pp. 233–343.

39. H. Thurn, *Kol. Z.*, **165**, 140 (1959). a. Dr. L. Brown, NMR Spectroscopist, Michigan Molecular Institute, private communication.

40. S. Beret and J. J. Prausnitz, *Macromolecules*, **8**, 536 (1975).

41. R. F. Boyer and R. L. Miller, *Macromolecules*, **17**, 365 (1984).

42. D. E. Axelson and L. Mandelkern, *J. Polym. Sci., Polym. Phys. Ed.*, **16**, 1135 (1978).

43. B. Stoll, W. Pechhold and S. Blasenbrey, *Kol. Z. u. Z. Polymere*, **250**, 1111 (1972).

44. K. Schmieder and K. Wolf, *Kol. Z.*, **134**, 149 (1953).

45. E. R. Fitzgerald, L. D. Grandine, Jr, and J. D. Ferry, *J. Appl. Phys.*, **24**, 650 (1953).

46. J. D. Ferry, L. D. Grandine, and E. R. Fitzgerald, *J. Appl. Phys.*, **24**, 911 (1953).

47. J. F. Sanders and J. D. Ferry, *Macromolecules*, **7**, 681 (1974).

48. R. H. Valentine, J. D. Ferry, T. Homa, and K. Ninomya, *J. Poly. Sci. A-2*, **6**, 479 (1968).

49. *Polymer Handbook*, Second Edition, Section IV, "Chain Stiffness," Wiley and Sons, New York 1975, pp. 33ff.

50. O. Kramer, R. Greco, R. A. Neira, and J. D. Ferry, *J. Poly. Sci., Polym. Phys. Ed.*, **12**, 2361 (1974).

51. L. M. Wei, B. S. Thesis on Torsional Braid Analysis of PIB, Dept. of Chemical Eng., Princeton Univ, May 1978, J. K. Gillham, thesis supervisor.

52. S. J. Stadnicki, J. K. Gillham, and R. F. Boyer, *J. Appl. Polym. Sci.*, **20**, 1245 (1976).

53. L. E. Nielsen, *Polym. Eng. Sci.*, **17**, 713 (1974).

54. N. G. McCrum, B. E. Read, and G. Williams, *Anelastic and Dielectric Effects in Polymer Solids*, Wiley, New York, 1967.

55. Dr. H. W. Starkweather, Experimental Station, E. I. duPont de Nemours, Wilmington, Delaware, advised RFB that he now finds the loss signal from the DMA to be numerically equivalent to G″ rather than to tan δ.

56. J. R. Martin and J. K. Gillham, *J. Appl. Polym. Sci.*, **16**, 2091 (1973).

57. J. D. Ferry and G. S. Parks, *Physics*, **6**, 365 (1935).

58. T. G. Fox and P. J. Flory, *J. Am. Chem. Soc.*, **70**, 2384 (1948).

59. H. Hendus, G. Schnell H. Thurn, and K. Wolf, *Ergebn. exakt. Naturwiss*, **31**, 220 (1959). This reprints the PIB results in Ref. 39 but somewhat more elaborately.

60. W. P. Slichter, *J. Poly. Sci.*, **C14**, 33 (1966).

61. D. W. McCall, "Relaxation in Solid Polymers," in *Molecular Dynamics and Structure of Solids*, R. S. Carter and J. J. Rush, Eds. National Bureau of Standards, Special Publication 301, June 1969.

62. G. P. Mikhaelov, T. I. Borosova, N. N. Ivanov, and A. S. Nigmankhodzhayev, *Poly. Sci. USSR*, **9**, 869 (1967). (Does not cover PIB.)

63. G. D. Patterson, *J. Polym. Sci., Polym. Phys. Ed.*, **15**, 455 (1977).

64. P. M. Smith, R. F. Boyer and P. L. Kumler, *Macromolecules*, **12**, 61 (1979).

65. P. M. Smith, *Europ. Polym. J.*, **15**, 147 (1979).

66. J. F. Sanders and J. D. Ferry, *Macromolecules*, **7**, 681 (1974), Figure 7 and Table II.

67. J. R. Stevens and R. M. Rowe, *J. Appl. Phys.*, **44**, 4328 (1973).

68. G. D. Patterson, H. E. Bair, and A. E. Tonelli, *J. Polym. Sci., Polym. Symp. Ed.*, **54**, 249 (1979).

69. D. J. Plazek, *J. Polym. Sci., Polym. Phys. Ed.*, **20**, 1533 (1982).

70. R. M. Neumann and W. J. MacKnight, *J. Polym. Sci., Polym. Phys. Ed.*, **19**, 369 (1981).

71. a. D. J. Plazek and G.-F. Gu, *J. Polym. Sci. Polym. Phys. Ed.*, **20**, 1551 (1982). b. J. Chen, C. Kow, L. J. Fetters and D. J. Plazek, *J. Poly. Sci., Polym. Phys. Ed.*, **20**, 1565 (1982). c. S. J. Orbon and D. J. Plazek, *J. Polym. Sci., Polym. Phys. Ed.*, **20**, 1575 (1982).

72. R. F. Boyer, *J. Polym. Sci., Polym. Symp. Ed.*, **C-14**, Preface (1966).

73. K. Ueberreiter, *Kolloid Z.*, **102**, 272 (1943).

74. V. A. Kargin and T. I. Sogolova, *Zhur. Fiz. Khim. (USSR)*, **23**, 530 (1949). *Chem. Abstr.*, **43**, 7294. See Refs. 75 and 76 below.

75. A professional English translation of this article is available from PK Translation Co., 5290 E Southern Avenue, Apache Junction, AZ 85220. Price on request, attention P. K. Fischer.

76. For a description of the penetrometer technique, see W. Kargin and G. Slonimsky, *Ency. Polym. Sci. Techn.*, N. Bikales Ed., Wiley Interscience, Section on Mechanical Properties.

77. R. F. Boyer and R. L. Miller, *Rubber Chem. Techn.*, **51**, 718 (1978) Table II.

78. K. Ueberreiter and H.-J. Orthmann, *Kunststoffe*, **48**, 525 (1958).

79. R. F. Boyer, *Macromolecules*, **7**, 142 (1974).

80. L. R. G. Treloar, *Physics of Rubber Elasticity*, 2nd ed., Oxford Press, 1958; 3rd ed., Claredon Press, Oxford, 1975, Fig. 1.5, p. 15.

81. T. Raphael and C. D. Armeniades, *Polym. Eng. Sci.*, **7**, 21–24 (1967).

82. O. Kramer and J. D. Ferry, in *Science and Technology of Rubber*, F. R. Eirich, Ed., Academic Press, New York, 1978, Chapter 5, p. 179ff, esp. pp. 201, 207.

83. *Polysar Handbook*, Polymer Corp., Sarnia, Ontario Canada courtesy Dr. B. M. E. VanderHoff, circa 1969.

84. B. Maxwell and K. S. Cook, J. Poly Sci. Polymer Symposium **72**, 343 (1985).

85. B. Maxwell, Abstract G-6, Soc. Rheology 55th Annual Meeting, Knoxville, Tenn., Oct. 17–20, 1983.

Received July 1, 1985
Accepted October 15, 1985